Inorganic Chemistry

Article

pubs.acs.org/IC

Reactivity of a Tin(II) (Iminophosphinoyl)(thiophosphinoyl)-methanediide Complex Toward Sulfur: Synthesis and ^{119}Sn Mössbauer Spectroscopic Studies of $[\{(\mu\text{-S})SnC(PPh_2{=}NSiMe_3)(PPh_2{=}S)\}_3Sn(\mu_3\text{-S})]$

Jia-Yi Guo,[†] Hong-Wei Xi,[§] Israel Nowik,[‡] Rolfe H. Herber,*[,‡] Yongxin Li,[†] Kok Hwa Lim,[§] and Cheuk-Wai So*[,†]

[†]Division of Chemistry and Biological Chemistry, School of Physical and Mathematical Sciences, Nanyang Technological University, 21 Nanyang Link, 637371 Singapore

[‡]Racah Institute of Physics, The Hebrew University of Jerusalem, Kaplun 23, 91904 Jerusalem, Israel

[§]Division of Chemical and Biomolecular Engineering, School of Chemical and Biomedical Engineering, Nanyang Technological University, 62 Nanyang Drive, 637459 Singapore

Supporting Information

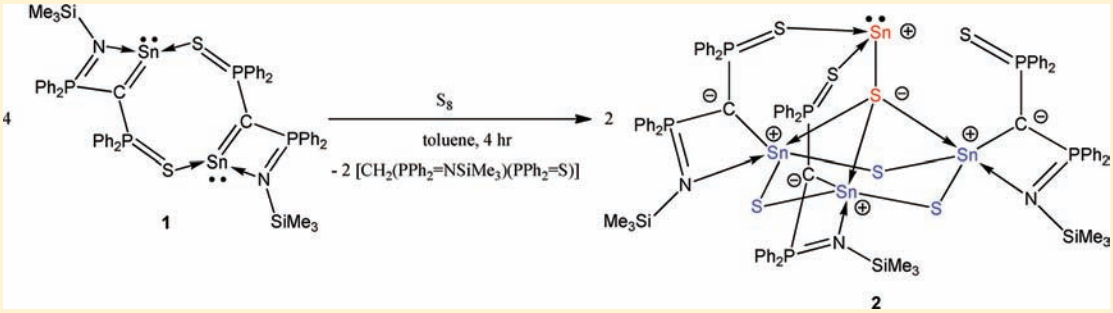

ABSTRACT: Reaction of $[(PPh_2{=}NSiMe_3)(PPh_2{=}S)CSn{:}]_2$ (**1**) with elemental sulfur in toluene afforded $[\{(\mu\text{-S})Sn^{IV}C(PPh_2{=}NSiMe_3)(PPh_2{=}S)\}_3Sn^{II}(\mu_3\text{-S})]$ (**2**) and $[CH_2(PPh_2{=}NSiMe_3)(PPh_2{=}S)]$ (**3**). Compound **2** comprises a $Sn^{II}S$ moiety coordinated with the Sn^{IV} and S atoms of a trimeric 2-stannathiomethendiide $\{(PPh_2{=}NSiMe_3)(PPh_2{=}S)CSn(\mu\text{-S})\}_3$. Compound **2** has been characterized by NMR spectroscopy, ^{119}Sn Mössbauer studies, X-ray crystallography, and theoretical studies. ^{119}Sn NMR spectroscopy and Mössbauer studies show the presence of Sn^{IV} and Sn^{II} atoms in **2**. X-ray crystallography suggests that the $Sn^{II}S$ moiety does not have multiple bond character. Theoretical studies illustrate that the $C_{methanediide}$–Sn bonds comprise a lone pair orbital on each $C_{methanediide}$ atom and an C–Sn occupied σ orbital.

INTRODUCTION

Tin(II) sulfide (SnS) occurs naturally as herzenbergite. At room temperature, it adopts a distorted rock-salt layered structure. Each tin atom in herzenbergite forms three short Sn–S bonds (2.7 Å) within the layer and three long Sn–S bonds (3.4 Å) connecting two neighboring SnS layers.[1] Moreover, there is a lone pair of electrons ($5s^2$) at each tin atom. Since SnS has a narrow band gap of 1.3 eV, its thin films and nanocrystals have been synthesized and investigated extensively as holographic recording systems, solar control devices, and photovoltaic materials.[2] In contrast, a stable monomeric tin(II) sulfide molecule, which is the heavier analogue of carbon monoxide, is still unknown. Recently, several research groups demonstrated that reactive species can be stabilized by forming an adduct with both Lewis acid and Lewis base.[3] For example, Rivard et al. reported that the heavier ethylene analogues $[IPr \rightarrow Si(H_2){-}E(H_2) \rightarrow W(CO)_5]$ (IPr = $\{HCN(2,6\text{-}Pr^i_2C_6H_3)\}_2C{:}$, E = Ge or Sn) are stabilized by a N-heterocyclic carbene (Lewis base) and $W(CO)_5$ (Lewis acid).[3a] Moreover, Hahn et al. showed that a SnO moiety can be trapped by a lutidene-bridged bisstannylene during reaction of the bistannylene with water.[3g] We anticipate that a monomeric tin(II) sulfide moiety could be isolable by coordinating the tin and sulfur atoms with suitable Lewis acid and base.

Recently, we reported the synthesis and characterization of a tin(II) methanediide complex $[(PPh_2{=}NSiMe_3)(PPh_2{=}S)CSn{:}]_2$ (**1**).[4] X-ray crystallography and DFT calculations suggest that the Sn–C bond in compound **1** has a >C=Sn: skeleton, which is stabilized by the lone pair of electrons on the nitrogen and sulfur donors. In this paper, we describe the reaction of **1** with elemental sulfur to form

Received: September 7, 2011
Published: March 12, 2012

   dx.doi.org/10.1021/ic2019633 | *Inorg. Chem.* 2012, 51, 3996–4001

$[\{(\mu\text{-S})Sn^{IV}C(PPh_2{=}NSiMe_3)(PPh_2{=}S)\}_3Sn^{II}(\mu_3\text{-S})]$ (**2**). Compound **2** comprises a $Sn^{II}S$ moiety coordinated with the Sn^{IV} and S atoms of a trimeric 2-stannathiomethendiide $\{(PPh_2{=}NSiMe_3)(PPh_2{=}S)CSn(\mu\text{-S})\}_3$. ^{119}Sn Mössbauer spectroscopic studies of **2** were also performed to identify the oxidation states of tin atoms. For clarity, the tin(IV) atoms of **2** are labeled as Sn(1), Sn(2), and Sn(3), while the tin(II) atom is labeled as Sn(4).

RESULTS AND DISCUSSION

Synthesis of $[\{(\mu\text{-S})Sn^{IV}C(PPh_2{=}NSiMe_3)(PPh_2{=}S)\}_3Sn^{II}(\mu_3\text{-S})]$ (2). Reaction of **1** with elemental sulfur in toluene for 4 h afforded a mixture of $[\{(\mu\text{-S})Sn^{IV}C(PPh_2{=}NSiMe_3)(PPh_2{=}S)\}_3Sn^{II}(\mu_3\text{-S})]$ (**2**), $[CH_2(PPh_2{=}NSiMe_3)(PPh_2{=}S)]$ (**3**),[5] and unidentified minor products, which was confirmed by NMR spectroscopy (Scheme 1). Pure compound

Scheme 1. Synthesis of 2 and 3

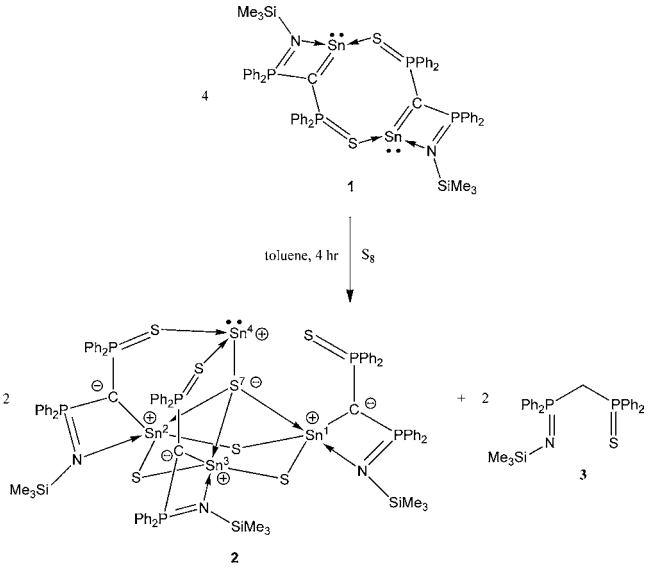

2 can be isolated as orange crystals in 29.2% yield by recrystallization in toluene. The reaction appears to proceed through an oxidative addition of **1** with elemental sulfur to form an unstable 2-stannathiomethendiide intermediate "$(PPh_2{=}NSiMe_3)(PPh_2{=}S)CSn{=}S$", which then decomposes to form intermediates "$(PPh_2{=}NSiMe_3)(PPh_2{=}S)C$:" and "SnS". A monomeric SnS moiety is trapped by the Sn^{IV} and S atoms of a trimeric 2-stannathiomethendiide $\{(PPh_2{=}NSiMe_3)(PPh_2{=}S)CSn(\mu\text{-S})\}_3$ to form **2**. Subsequently, **3** could be formed by hydrogen abstraction of "$(PPh_2{=}NSiMe_3)(PPh_2{=}S)C$:" with the solvents. Chivers et al. reported that the intermediate $[:C(PPh_2{=}S)_2]$ dimerizes to form $[(SPh_2P)_2C_2(PPh_2)_2S_2]$, which contains a six-membered $C_2P_2S_2$ ring.[6] However, dimerization of "$(PPh_2{=}NSiMe_3)(PPh_2{=}S)C$:" cannot be observed in the reaction of **1** with elemental sulfur in toluene; instead, compound **3** was formed. Moreover, when the reaction of **1** with elemental sulfur was performed in THF for 20 min, a mixture of **2** and **3** can be isolated in a ratio of 1:1, which was confirmed by NMR spectroscopy. The results illustrate that decomposition of "$(PPh_2{=}NSiMe_3)(PPh_2{=}S)CSn{=}S$" and hydrogen abstraction of "$(PPh_2{=}NSiMe_3)(PPh_2{=}S)C$:" are enhanced in a polar solvent. Compound **2** is stable in the solid state at room temperature under an inert atmosphere. Orange crystals of **2** are soluble in CH_2Cl_2 only, and it decomposes slowly in solution to give **3**. Compound **2** can be considered as an intermediate during decomposition of the unstable 2-stannathiomethendiide intermediate "$(PPh_2{=}NSiMe_3)(PPh_2{=}S)CSn{=}S$". Thus, when the reaction of **1** with elemental sulfur in toluene was performed overnight, only compound **3** formed.

A freshly prepared solution of **2** in CD_2Cl_2 was characterized by NMR spectroscopy. The ^{1}H NMR spectrum shows one singlet (δ −0.29 ppm) and multiplets (δ 6.88−7.38 ppm) for the $SiMe_3$ and phenyl protons, respectively. In the molecular structure of **2** (Figure 3), the S(1−3) atoms have similar orientation toward the Sn(4) atom but the Sn(4)−S(2−3) bond lengths are shorter than the Sn(4)···S(1) distance. These lead to nonequivalent P(2,4,6) atoms. However, the $^{31}P\{^1H\}$ NMR spectrum at room temperature or −60 °C shows two doublets at δ 27.42 and 30.07 ppm, which correspond to two nonequivalent phosphorus nuclei. The results are not consistent with the solid-state structure. These indicate that the thiophosphinoyl substituents are fluxional in solution or the S(1−3) atoms may be equivalent in solution with equal Sn(4)···S(1−3) distances. The $^{119}Sn\{^1H\}$ NMR spectrum of **2** at room temperature or −60 °C shows a multiplet at δ −242.1 ppm. ^{119}Sn solid-state NMR spectroscopy was performed. The ^{119}Sn CPMAS NMR signals (δ_{iso} = −260.3 (Sn(4)), −232.3 ppm (Sn(1−3)) show two nonequivalent tin environments in **2**. The isotropic chemical shift for the Sn(1−3) atoms (δ_{iso} = −232.3 ppm) shows an upfield shift compared with the ^{119}Sn NMR signal of $[Sn\{N(SiMe_3)_2\}_2(\mu\text{-S})]_2$ (δ −106.6 ppm).[7] The isotropic chemical shift for the Sn(4) atom (δ_{iso} = −260.3 ppm) shows an upfield shift compared with the ^{119}Sn NMR signal of SnO trapped by the lutidene-bridged bisstannylene (δ −85.1 ppm).[3g]

Temperature-Dependent ^{119}Sn Mössbauer (ME) Studies. ME spectra of **2** were examined over the range $5.5 < T < 181$ K and give evidence of three distinct tin sites. As usual, these resonances consist of well-resolved doublets, and a typical spectrum at 91.7 K is shown in Figure 1. As will be noted the

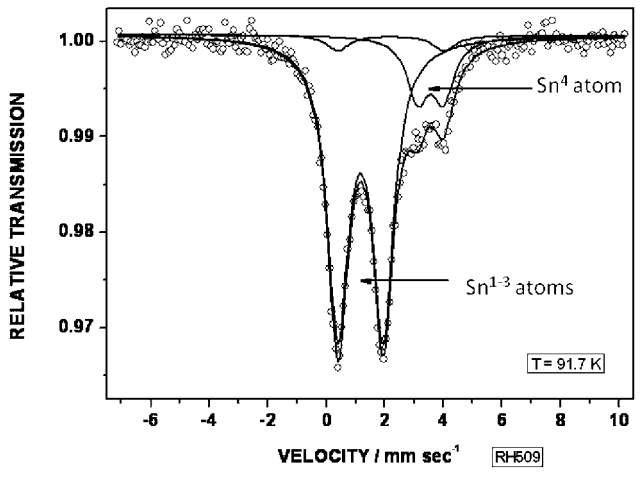

Figure 1. ^{119}Sn Mössbauer spectrum of compound **2** at 91.7 K.

spectrum consists of a major resonance at an isomer shift (IS) of about 1.17 mm s^{-1}, a second absorbance at an IS of about 3.56 mm s^{-1}, and a third site at an IS of about 2.2 mm s^{-1}, all with respect to the room-temperature $BaSnO_3$ reference point. The major site is clearly due to Sn(IV), while the second resonance arises from a Sn(II) site. The hyperfine interaction

dx.doi.org/10.1021/ic2019633 | Inorg. Chem. 2012, 51, 3996−4001

parameters (IS and QS) of these two sites at 91.7 K are summarized in Table 1. These hyperfine parameters are unfortunately

Table 1. ^{119}Sn Mössbauer Spectroscopic Data of 2 at 91.7 K[a]

atom	IS	QS	Γ	formal oxidation state	I_R
Sn(4)	3.57(3)	0.87(2)	0.84(7)	+II	0.203
Sn(1−3)	1.170(4)	1.550(4)	0.87(1)	+IV	1.00

[a]IS: isomer shift (mm s^{-1}). QS: electric quadrupole splitting (mm s^{-1}). Γ: experimental line width (mm s^{-1}). I_R: relative intensity.

not sufficiently temperature sensitive to permit a meaningful calculation of the effective mass and ME lattice temperature, since the recoil-free fraction, *f*, becomes very small above about 200 K. The chemical identity of the third resonance (amounting to about 4% of the total area at 91.7 K) cannot be identified from the present data. However, the temperature dependence of the *f* parameter, which is given by the temperature dependence of the area under the resonance curve for an optically thin absorber, is determinable. For the Sn(1−3) atoms, $(-\mathrm{d}\ln A)/\mathrm{d}T = 20.5(2) \times 10^{-3}$ with a correlation coefficient of 0.986 for 10 data points. For the Sn(4) atom, $(-\mathrm{d}\ln A)/\mathrm{d}T = 24.9(2) \times 10^{-3}$ with a correlation coefficient of 0.96 for 10 data points. These data are summarized graphically in Figure 2 in terms of

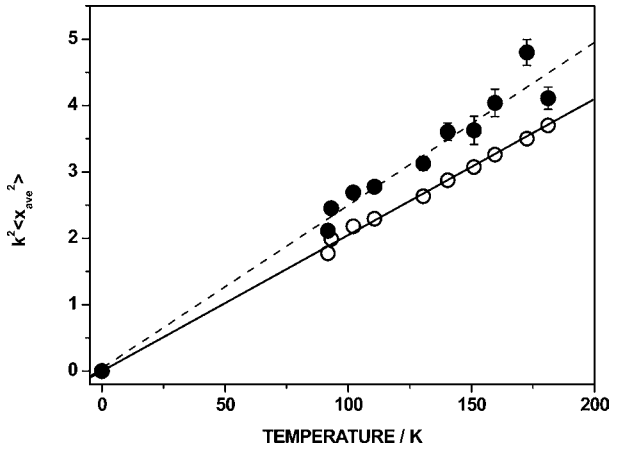

Figure 2. Temperature dependence of the *F* parameter for the Sn(1−3) atoms (○) and the Sn(4) atom (●) of **2**.

the parameter $F = k^2\langle x_{ave}{}^2\rangle$, vide infra, from which it is clear that the Sn(II) site is significantly softer than the Sn(IV) sites.

This observation is also consistent with the temperature dependence of the area ratio of the two sites, $R = A_{Sn(4)}/A_{Sn(1-3)}$ which decreases with increasing temperature due to the difference in the temperature dependence of the recoil-free fractions as referred to above.

To focus on the metal atom dynamics in **2**, the U_{ij} values extracted from the single-crystal X-ray data (see the Supporting Information) have been used to evaluate the mean square amplitude of vibration (msav) of the Sn atoms and compare this to the value extracted from the temperature-dependent ME data, as described previously.[8] The msav is best expressed in terms of the *F* parameter, where $F = k^2\langle x_{ave}{}^2\rangle$ and k^2 is the square of the ME gamma-ray wave vector (1.464×10^{18} cm^2). The values so calculated are $F_{X,103} = 2.78 \pm 0.12$ for the Sn(1−3) atoms and $F_{M,103} = 2.11 \pm 0.21$. For the Sn(4) atom, $F_{X,103} = 3.66 \pm 0.12$ and $F_{M,103} = 2.57 \pm 0.26$, all at 103 K, where the X and M subscripts indicate the X-ray- and ME-derived values, respectively. Again, the msav data for the Sn(4) atom indicate a significantly larger value than those for the Sn(1−3) atoms, consistent with the dynamical data referred to above. As noted previously for ^{119}Sn data,[9] the *F* values derived from the ME data are consistently smaller than those derived from the X-ray values, and the differences are presumed to arise from the presence of crystal lattice imperfections and/or the presence of low-lying librational and torsional motions of the metal atom, which are slow on the ME time scale but cumulatively averaged in the X-ray data. Again, these observations are consistent with a softer metal atom−S ligation in the case of the Sn(4) atom than in the case of the Sn(1−3) atoms as indicated above.

X-ray Crystal Structure of 2. Single crystals suitable for X-ray crystallography were obtained by recrystallization of **2** in C_6D_6. The molecular structure of **2** is shown in Figure 3. Phenyl substituents and disordered solvent molecules are omitted for clarity in the figure. The numbering scheme of tin atoms in the molecular structure is same as in Scheme 1. Selected bond lengths and angles of **2** are shown in Table 2.

Table 2. Selected Bond Lengths (Angstroms) and Angles (degrees) of Compound 2

Sn(4)−S(7)	2.6119(19)	Sn(4)−S(2)	2.686(3)
Sn(4)−S(3)	2.813(3)	Sn(1)−S(7)	2.6771(19)
Sn(2)−S(7)	2.678(2)	Sn(3)−S(7)	2.659(2)
Sn(1)−S(4)	2.407(2)	Sn(1)−S(5)	2.410(2)
Sn(2)−S(4)	2.412(2)	Sn(2)−S(6)	2.404(2)
Sn(3)−S(5)	2.415(2)	Sn(3)−S(6)	2.412(2)
C(1)−Sn(1)	2.104(8)	C(1)−P(1)	1.717(8)
C(1)−P(2)	1.698(8)	P(1)−N(1)	1.612(7)
P(2)−S(1)	2.015(3)	N(1)−Sn(1)	2.223(6)
C(29)−Sn(2)	2.119(7)	C(29)−P(3)	1.722(8)
C(29)−P(4)	1.701(8)	P(3)−N(2)	1.620(7)
P(4)−S(2)	2.031(3)	N(2)−Sn(2)	2.217(7)
C(57)−Sn(3)	2.119(8)	C(57)−P(5)	1.722(8)
C(57)−P(6)	1.697(8)	P(5)−N(3)	1.606(7)
P(6)−S(3)	2.011(3)	N(3)−Sn(3)	2.250(7)
Sn(4)···S(1)	2.920(2)		
S(2)−Sn(4)−S(3)	106.75(8)	S(2)−Sn(4)−S(7)	88.53(7)
S(3)−Sn(4)−S(7)	88.51(7)	Sn(4)−S(7)−Sn(1)	127.97(8)
Sn(4)−S(7)−Sn(2)	129.63(8)	Sn(4)−S(7)−Sn(3)	129.95(8)
S(4)−Sn(1)−S(5)	114.63(8)	Sn(1)−S(5)−Sn(3)	96.34(7)
S(5)−Sn(3)−S(6)	113.49(7)	Sn(3)−S(6)−Sn(2)	95.66(7)
S(6)−Sn(2)−S(4)	111.41(7)	Sn(2)−S(4)−Sn(1)	96.49(7)
P(1)−C(1)−P(2)	136.6(5)	P(1)−C(1)−Sn(1)	94.3(3)
P(2)−C(1)−Sn(1)	128.8(4)	P(3)−C(29)−P(4)	133.3(5)
P(3)−C(29)−Sn(2)	93.8(3)	P(4)−C(29)−Sn(2)	130.1(4)
P(5)−C(57)−P(6)	134.7(5)	P(5)−C(57)−Sn(3)	93.8(4)
P(6)−C(57)−Sn(3)	130.3(5)		

The methanediide ligands are coordinated in a *C,N*-chelate fashion to the Sn(1), Sn(2), and Sn(3) atoms, which adopt a distorted trigonal bipyramidal geometry. The C(1)−Sn(1) (2.104(8) Å), C(29)−Sn(2) (2.119(7) Å), and C(57)−Sn(3) (2.119(8) Å) bonds are shorter than that in **1** (2.199(4) Å) and

dx.doi.org/10.1021/ic2019633 | Inorg. Chem. 2012, 51, 3996−4001

the 1,3-distannacyclobutane $[Sn\{\mu^2\text{-}C(PPh_2{=}NSiMe_3)_2\}]_2$ (average 2.322 Å).[10] The Sn(1)−N(1) (2.223(6) Å), Sn(2)−N(2) (2.217(7) Å), and Sn(3)−N(3) (2.250(7) Å) bonds in **2** are comparable with that in **1** (2.2554(8) Å). Moreover, they are longer than the terminal Sn−N σ bond in $[:Sn\{N(SiMe_3)_2\}_2]$ (2.088(6), 2.096(1) Å).[11] The S(4), S(5), and S(6) atoms are bridged between the Sn(1), Sn(2), and Sn(3) atoms. The Sn−S(4), Sn−S(5), and Sn−S(6) bonds (2.404(2)−2.415(2) Å) are comparable with the Sn−S single bonds in $[(Tbt)(Mes)Sn(\mu\text{-}S)]_2$ (Tbt = 2,4,6-$\{CH(SiMe_3)_2\}_3C_6H_2$, 2.434(3) and 2.432(3) Å)[12] and $[Sn\{N(SiMe_3)_2\}_2(\mu\text{-}S)]_2$ (2.416(5) and 2.413(6) Å).[7] In addition, the S(1−3) atoms of the thiophosphinoyl substituents have a similar orientation toward the Sn(4) atom. It is noteworthy that the S(1)···Sn(4) distance (2.920(2) Å) is significantly longer than the S(2)−Sn(4) (2.686(3) Å) and S(3)−Sn(4) bond lengths (2.813(3) Å), but the S(1)···Sn(4) distance is shorter than the sum of van der Waals' radii (ca. 4 Å). This suggests that there is a weak interaction between the S(1) and the Sn(4) atoms. The S(7)−Sn(4)−S(2) and S(7)−Sn(4)−S(3) angles are almost 90°, which imply that the Sn(4) atom possesses high-s-character lone pairs (see below). The Sn(4)−S(7) bond (2.6119(19) Å) is significantly longer than the Sn−S single bonds in $[(Tbt)(Mes)Sn(\mu\text{-}S)]_2$ (2.434(3) and 2.432(3) Å)[12] and $[Sn\{N(SiMe_3)_2\}_2(\mu\text{-}S)]_2$ (2.416(5) and 2.413(6) Å),[7] which indicates that there is no multiple-bond character between the Sn(4) and the S(7) atoms (see below). Furthermore, the geometry around the S(7) atom is tetrahedral. These imply that there are three lone pairs of electrons on the S(7) atom for formation of the S(7)−Sn(1−3) bonds (2.659(2)−2.678(2) Å).

Theoretical Studies of 2. In order to understand the bonding nature in compound **2**, it was investigated by DFT calculations.[13] The optimized geometry of **2** (B3PW91/LANL08d for Sn, 6-31+G(d) for $C_{methanediide}$, N, P, S and Si, 6-31G(d) for C and H level) is in good agreement with the X-ray crystallographic data except the Sn(4)···S(1) distance and S(2)−Sn(4)−S(3) angle (Figure S1 with selected bond lengths and angles, see the Supporting Information). It is proposed that the crystal packing force leads to a stronger Sn(4)···S(1) interaction and hence a smaller S(2)−Sn(4)−S(3) angle in the X-ray crystal structure of **2** (Figure 3).

The natural bond orbital (NBO) analysis (Table S1, see the Supporting Information)[14] of **2** shows that there is a lone pair of electrons at the Sn(4) atom. The percentage of the s character of the lone pair orbital is high (93.5%). The Sn(4)−S(7) bond comprises an occupied σ orbital (electron occupancy = 1.98) only. It is formed by the overlapping of a $sp^{21.93}$ hybrid with 95.3% p character on the Sn(4) atom and a $sp^{1.85}$ hybrid on the S(7) atom. The results indicate that there is no multiple-bond character between the Sn(4) and the S(7) atoms. Moreover, the Sn(4)−S(2) bond is formed by the overlapping of a $sp^{59.07}$ hybrid with 97.85% p character on the Sn(4) atom and a $sp^{5.69}$ hybrid on the S(2) atom. The Sn(4)−S(3) bond is formed by the overlapping of a p orbital on the Sn(4) atom and a $sp^{5.99}$ hybrid on the S(3) atom. The results are consistent with the X-ray crystallographic data that the S(7)−Sn(4)−S(2) and S(7)−Sn(4)−S(3) angles are almost 90°.

In addition, NBO analysis shows that the $C_{methanediide}$−Sn bonds (C(1)−Sn(1), C(29)−Sn(2), C(57)−Sn(3)) comprise a lone pair orbital (LP) on each $C_{methanediide}$ atom and an C−Sn occupied σ orbital. The LP(C(1)), LP(C(29)), and LP(C(57)) are p orbitals which are stabilized by forming p−σ* negative

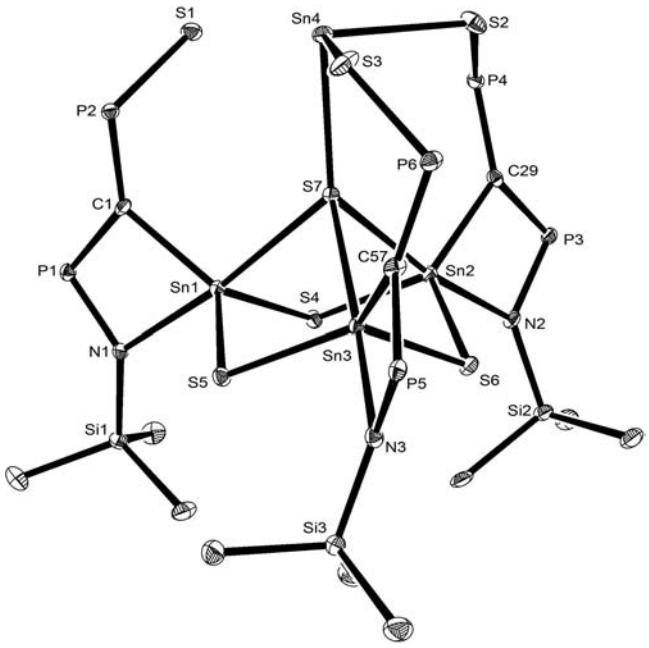

Figure 3. Molecular structure of **2** with thermal ellipsoids at the 20% probability level. Phenyl substituents, disordered solvent molecules, and hydrogen atoms are omitted for clarity.

hyperconjugation with the σ*(P−C), σ*(P−S), and σ*(Sn−S) orbitals (stabilizing energy = 61.16 kcal mol^{-1} for LP(C(1)), 60.52 kcal mol^{-1} for LP(C(29)), and 60.03 kcal mol^{-1} for LP(C(57)), Table S3, Supporting Information). The Sn(1)−C(1), Sn(2)−C(29), and Sn(3)−C(57) bonds are highly polarized toward the $C_{methanediide}$ atoms (Sn(1)−C(1) bond = 81.3%, Sn(2)−C(29) = 81.9%, Sn(3)−C(57) = 81.6% polarization). Moreover, the NPA charges (Table S2, Supporting Information) of the $C_{methanediide}$ (−1.71 to −1.73) and Sn(1−3) atoms (1.89−1.90) indicate that the bonding between the $C_{methanediide}$ atoms and the tin(IV) atoms is highly ionic.

Furthermore, NBO analysis shows that the P−C, P−S, and P−N bonds are single bonds (Wiberg bond index (WBI)[15] of P−C, 1.02−1.06; P−N, 0.95; P−S, 1.08−1.18). Together with the NPA charges of the $C_{methanediide}$, P(1−6), N(1−3), and S(1−3) atoms (Table S2, Supporting Information), the methanediide ligand is best described as the structure **A** (Scheme 2).

Scheme 2. Resonance Structure A of the Methanediide Ligand

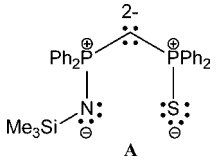

Accordingly, the S(2) and S(3) atoms donate one of the lone pair electrons to the Sn(4) atom, while the N(1−3) atoms donate one of the lone pair electrons to the Sn(1−3) atoms, respectively. As a result, there are one LP (p orbital) remaining on the N(1−3) atoms, two LPs remaining on the S(2−3) atoms (S(2) $sp^{0.43}$, p; S(3) $sp^{0.44}$, p), and three LPs ($sp^{0.28}$, p, $sp^{16.73}$) remaining on the S(1) atom (Table S1,

dx.doi.org/10.1021/ic2019633 | Inorg. Chem. 2012, 51, 3996−4001

Supporting Information). Thus, the theoretical studies are consistent with the X-ray crystallographic data of **2**.

In conclusion, reaction of $[(PPh_2{=}NSiMe_3)(PPh_2{=}S)CSn{:}]$ (**1**) with elemental sulfur in toluene afforded $[\{(\mu\text{-}S)Sn^{IV}C(PPh_2{=}NSiMe_3)(PPh_2{=}S)\}_3Sn^{II}(\mu_3\text{-}S)]$ (**2**), which comprises a SnS moiety coordinated with a trimeric 2-stannathiomethanediide $\{(PPh_2{=}NSiMe_3)(PPh_2{=}S)CSn(\mu\text{-}S)\}_3$. It was characterized by NMR spectroscopy, Mössbauer spectroscopy, X-ray crystallography, and theoretical studies. Conversion of compound **2** into SnS thin film or nanocrystal is currently under investigation.

EXPERIMENTAL SECTION

All manipulations were carried out under an inert atmosphere of nitrogen gas using standard Schlenk techniques. Solvents were dried and distilled over Na/K alloy prior to use. **1** was prepared as described in the literature.[4] The ^{1}H, ^{13}C, ^{31}P, ^{119}Sn, and ^{119}Sn CPMAS NMR spectra were recorded on a JEOL ECA 400 spectrometer. NMR spectra were recorded in CD_2Cl_2. The chemical shifts δ are relative to $SiMe_4$ for ^{1}H and ^{13}C and $SnMe_4$ for ^{119}Sn and H_3PO_4 for ^{31}P. Elemental analyses were performed by the Division of Chemistry and Biological Chemistry, Nanyang Technological University. Melting points were measured in sealed glass tubes and not corrected.

Synthesis of $[\{(\mu\text{-}S)Sn^{IV}C(PPh_2{=}NSiMe_3)(PPh_2{=}S)\}_3Sn^{II}(\mu_3\text{-}S)]$ (2). A solution of S_8 (0.013 g, 0.05 mmol) in toluene (7 mL) was added dropwise to **1** (0.23 g, 0.19 mmol) in toluene (15 mL) at 0 °C. The yellow suspension was raised to room temperature and stirred for 4 h. The solution became red and clear. The resultant red solution was filtered and concentrated to afford **2** as orange crystals. Yield: 0.058 g (29.2%). Single crystals suitable for X-ray crystallography were obtained by recrystallization of compound **2** in C_6D_6. Mp. 186.7 °C. Anal. Calcd for $C_{84}H_{87}N_3P_6S_7Si_3Sn_4$: C, 47.86; H, 4.16; N, 1.99. Found: C, 47.52; H, 4.03; N, 1.65. ^{1}H NMR (399.5 Hz, 21.8 °C): δ = −0.29 (s, 27H, $SiMe_3$), 6.88−7.38 ppm (m, 60 H, Ph). $^{13}C\{^{1}H\}$ NMR (100.5 MHz, 21.7 °C): δ = 2.74 ($SiMe_3$), 128.45, 130.67, 130.85, 132.54−132.85 (m) ppm (Ph). $^{31}P\{^{1}H\}$ NMR (161.7 MHz, 21.9 °C): δ = 27.42 (d, $^{2}J_{P-P'}$ = 8.67 Hz), 30.07 ppm (d, $^{2}J_{P-P'}$ = 8.68 Hz). $^{119}Sn\{^{1}H\}$ NMR (149.0 MHz, 21.8 °C): δ = −242.1 ppm (m). ^{119}Sn CPMAS NMR (149.0 MHz, spinning speed = 9 kHz): δ_{iso} = −260.3 (Sn^{4}), −232.3 ppm (Sn^{1-3}).

X-ray Data Collection and Structural Refinement. Intensity data for compound **2** were collected using a Bruker APEX II diffractometer. The crystal of **2** was measured at 103(2) K. The structure was solved by direct phase determination (SHELXS-97) and refined for all data by full-matrix least-squares methods on F^2.[16] All non-hydrogen atoms were subjected to anisotropic refinement. Hydrogen atoms were generated geometrically and allowed to ride in their respective parent atoms; they were assigned appropriate isotopic thermal parameters and included in the structure factor calculations. X-ray crystallographic data is summarized in Table 3.

Mössbauer Spectroscopy. The air- and moisture-sensitive sample was received in a sealed ampule which was opened in an inert atmosphere glovebox and the powder transferred to an O-ring-sealed Perspex sample holder which was immediately cooled to liquid nitrogen temperature. The sample was then transferred to the precooled cryostat and examined in transmission geometry using a $BaSnO_3$ source at room temperature. Temperature control and monitoring was effected as described earlier,[17] and all IS are referred to a $BaSnO_3$ room-temperature reference spectrum. Spectrometer calibration was derived from an α-Fe absorption spectrum at room temperature.

Table 3. Crystallographic Data for Compound 2

	2
formula	$C_{108}H_{87}D_{24}N_3P_6S_7Si_3Sn_4$
M	2444.41
color	orange
cryst syst	monoclinic
space group	$P2(1)/c$
a/Å	16.4619(10)
b/Å	33.693(2)
c/Å	19.8683(12)
α/deg	90
β/deg	92.672(4)
γ/deg	90
V /Å^3	11008.1(12)
Z	4
d_{calcd}/g cm^{-3}	1.475
μ/mm^{-1}	1.196
$F(000)$	4896
cryst size/mm	0.20 × 0.10 × 0.10
index range	$-21 \le h \le 21$
	$-44 \le k \le 45$
	$-25 \le l \le 26$
no. of reflns collected	147 130
$R1$, $wR2$ ($I > 2(\sigma)I$)	0.0770, 0.1862
$R1$, $wR2$ (all data)	0.1327, 0.2238
goodness of fit., F^2	1.176
no. of data/restraints/params.	27312/404/1235
largest diff. peak, hole/e Å^{-3}	1.860, −1.998

ASSOCIATED CONTENT

Supporting Information

Selected calculation results of **2**; CIF file giving X-ray data of **2**. This material is available free of charge via the Internet at http://pubs.acs.org.

AUTHOR INFORMATION

Corresponding Author

*E-mail: CWSo@ntu.edu.sg (C.-W.S.); herber@vms.huji.ac.il (R.H.H.).

Notes

The authors declare no competing financial interest.

ACKNOWLEDGMENTS

This work was supported by the Academic Research Fund Tier 1 (C.-W.S., RG 57/11; K.H.L., RG 28/07).

REFERENCES

(1) Wiedemeier, H.; von Schnering, H. G. *Z. Kristallogr.* **1978**, *148*, 295.

(2) For the synthesis of thin films and nanocrystals of SnS, see: (a) Bade, B. P.; Garje, S. S.; Niwate, Y. S.; Afzaal, M.; O'Brien, P. *Chem. Vap. Deposition* **2008**, *14*, 292 and references therein. (b) Malik, M. A.; Afzaal, M.; O'Brien, P. *Chem. Rev.* **2010**, *110*, 4417. (c) Antunez, P. D.; Buckley, J. J.; Brutchey, R. L. *Nanoscale* **2011**, *3*, 2399. For application of SnS, see: (d) Valiukonis, G.; Krivaite, D. G.; Sileica, A. *Phys. Status Solidi B* **1990**, *135*, 229. (e) Valiukonis, G.; Guseinova, D. A.; Krivaite, G.; Sileica, A. *Phys. Status Solidi B* **1986**, *135*, 299. (f) Parenteau, M.; Carlone, C. *Phys. Rev. B* **1990**, *41*, 5227. (g) Mondal, A.; Chaudhuri, T. K.; Pramanik, P. *Sol. Energy Mater.* **1983**, *7*, 431. (h) Johnson, J. B.; Jones, H.; Latham, B. S.; Parker, J. D.; Engelken, R. D.; Barber, C. *Semicond. Sci. Technol.* **1999**, *14*, 501. (i) Ray, S. C.; Karanjai, M. K.; DasGupta, D. *Thin Sol. Films* **1999**, *350*, 72.

(3) (a) Al-Rafia, S. M. I.; Malcolm, A. C.; McDonald, R.; Ferguson, M. J.; Rivard, E. *Angew. Chem., Int. Ed.* **2011**, *50*, 8354. (b) Al-Rafia, S. M. I.; Malcolm, A. C.; Liew, S. K.; Ferguson, M. J.; Rivard, E. *J. Am. Chem. Soc.* **2011**, *133*, 777. (c) Thimer, K. C.; Al-Rafia, S. M. I.; Ferguson, M. J.; McDonald, R.; Rivard, E. *Chem. Commun.* **2009**, 7119. (d) Abraham, M. Y.; Wang, Y.; Xie, Y.; Wei, P.; Schaefer, H. F. III; Schleyer, P. v. R.; Robinson, G. H. *J. Am. Chem. Soc.* **2011**, *133*, 8874. (e) Xiong, Y.; Yao, S.; Driess, M. *Angew. Chem., Int. Ed.* **2010**, *49*, 6642. (f) Wang, Y.; Hu, H.; Zhang, J.; Cui, C. *Angew. Chem., Int. Ed.* **2011**, *50*, 2816. (g) Zabula, A. V.; Pape, T.; Hepp, A.; Schappacher, F. M.; Rodewald, U. C.; Pöttgen, R.; Hahn, F. E. *J. Am. Chem. Soc.* **2008**, *130*, 5648. (h) Meltzer, A.; Inoue, S.; Präsang, C.; Driess, M. *J. Am. Chem. Soc.* **2010**, *132*, 3038.

(4) Guo, J.; Lau, K.-C.; Xi, H.-W.; Lim, K. H.; So, C.-W. *Chem. Commun.* **2010**, *46*, 1929.

(5) Chen, J.-H.; Guo, J.; Li, Y.; So, C.-W. *Organometallics* **2009**, *28*, 4617.

(6) Konu, J.; Chivers, T. *Chem. Commun.* **2008**, 4995.

(7) Hitchcock, P. B.; Jang, E.; Lappert, M. F. *J. Chem. Soc., Dalton Trans.* **1995**, 3179.

(8) Herber, R. H.; Nowik, I.; Mochida, T. *J. Organomet. Chem.* **2011**, *696*, 1698.

(9) (a) Mansell, S.; Herber, R. H.; Nowik, I.; Ross, D. H.; Russell, C. A.; Wass, D. F. *Inorg. Chem.* **2011**, *50*, 2252. (b) Herber, R. H.; Nowik, I. *Phosphorus, Sulfur Silicon* **2011**, *186*, 1336 and references therein.

(10) Leung, W.-P.; Wang, Z.-X.; Li, H.-W.; Mak, T. C. W. *Angew. Chem., Int. Ed.* **2001**, *40*, 2501.

(11) Fjeldberg, T.; Hope, H.; Lappert, M. F.; Power, P. P.; Thorne, A. J. *J. Chem. Soc., Chem. Commun.* **1983**, 639.

(12) Matsuhashi, Y.; Tokitoh, N.; Okazaki, R. *Organometallics* **1993**, *12*, 2573.

(13) For the details of theoretical studies and references, see the Supporting Information.

(14) Weinhold, F.; Landis, C. R. In *Valency and Bonding: A Natural Bond Orbital Donor-Acceptor Perspective*; Cambridge University Press: UK, 2005.

(15) Wiberg, K. B. *Tetrahedron* **1968**, *24*, 1083.

(16) Sheldrick, G. M. *SHELXL-97*; Universität Göttingen: Göttingen, Germany, 1997.

(17) Merrill, W. A.; Steiner, J.; Betzer, A.; Nowik, I.; Herber, R.; Power, P. P. *Dalton Trans.* **2008**, 5905 and references therein.